Electronic Supplementary Material (ESI) for Journal of Materials Chemistry A.

Electronic Supplementary Information

Imidazole-functionalized polyketone-based polyelectrolyte with efficient ionic channels and superwettability for alkaline polyelectrolyte fuel cell and multiple liquid purification

Yi-cun Zhou, Zheng-min Zhang, Ling Zhou, Rui-Ying Bao, Zheng-Ying Liu, Ming-Bo Yang, Wei Yang*

College of Polymer Science and Engineering, Sichuan University, State Key Laboratory of Polymer Materials Engineering, Chengdu, 610065, Sichuan, People's Republic of China.

1. Experimental section

1.1. Materials

The polyketone (PK) resin (M630A, Mw=100,000) with a density of 1.24 g/cm^3 was purchased from Hyosung Co., Ltd., (Seoul, Korea). Dichloromethane (DCM) and 1,1,1,3,3,3-hexafluoro-2-propanol (HFIP) were purchased from Aladdin Reagent Co. Ltd (Shanghai, China). Bismuth (III) nitrate pentahydrate (BNP), 3-aminopropyl-imidazole (API) and methyl iodide (MeI) were bought from Adamas-beta Reagent Co. Ltd (Shanghai, China). Sodium hydroxide (NaOH), potassium hydroxide (KOH), potassium chromate (K_2CrO_4), sodium sulfate (Na_2SO_4), silver nitrate ($AgNO_3$) and ethanol were supplied by Haihong Chemical Reagents Company (Chengdu, China). All solvents and reagents were directly employed as received without further purification. The deionized water was obtained from the deionized water generator (Sichuan Youpu Technology Co., Ltd. China).

1.2 Synthesis of quaternized imidazole-functionalized polyketone

The quaternized imidazole-functionalized polyketone was synthesized by bismuth

---

Corresponding author. Tel.: + 86 28 8546 0130; fax: + 86 28 8546 0130.

E-mail address: weiyang@scu.edu.cn (W Yang)

nitrate-catalyzed Paal-Knorr reaction and quaternarization of imidazole. Briefly, HFIP (20.6 ml, 31.1 g) and DCM (51.4 ml, 66.7 g) were uniformly mixed in a 250 mL round bottom flask reactor. PK resin (2.6 g) was added to solution, and the transparent solution was acquired after 30 min high-speed stirring at room temperature. The BNP (223.2 mg) was added to PK solution and was treated with sonication for 40s to get the PK solution with a uniformly dispersed BNP. The certain amount of API (115 μL, 165 μL, 250 μL, 319 μL and 386 μL) was added to the prepared solution, and it reacted at 35 ℃ for 15 hours under high-speed stirring. Afterward, MeI (1.3 mL) was dropwise added into the reactor with aluminum foil for shading treatment, and the reactor continued to react for 24 hours at 35 °C. In this experiment, the content of imidazole functional groups introduced into the PK molecular chain was controlled by the amount of API added. The reaction product was named as QAAPIPK-1-n (n = 8, 6, 5, 4 and 3), and 1-n represents the ratio of the structural unit with introduced imidazole functional groups in all 1, 4-dicarbonyl structural units of PK.

1.3. Fabrication of QAAPIPK based anion exchange membranes

The obtained solution of QAAPIPK was placed at -20 °C for 30 min. The BNP at the bottom of the solution was removed, and this operation was repeated 6-8 times. The resulting solution named QAAPIPK-1-n was poured into the membrane-frame with polytetrafluoroethylene material, and the thickness of the casting membrane was regulated by the amount of solution added. The solvent volatilization process was carried out in a fume hood at room temperature for 1-2 days, and the solvent-free membrane was named as QAAPIPK-1-n-C (n = 8, 6, 5, 4 and 3). The obtained membrane was immersed in a mixture of dichloromethane and ethanol for 24 hours, and the solution was changed several times during this process. After vacuum drying, the final membranes were obtained. The thickness of the membranes is controlled at 120-150 μm.

1.4. Fabrication of QAAPIPK based liquid separation membranes

The liquid separation membrane was fabricated by the electrospinning machine ET-2535H Nanosetup (Ucalery, China) using the spinning solution with the concentration of 2.5 wt%. The electrospinning conditions were as follows: the positive electrode voltage of 13.5 kV, the negative electrode voltage of 2.5 kV, the relative humidity of 35-45%, the electrospinning temperature of 25-29 °C, and the collection distance of 20 cm between the roller collector and the tip of the needle. The thickness of the electrospinning membrane was regulated by the spinning time. The resulting membranes were further dried to obtain the final sample and were called as QAAPIPK-1-n-E (n = 8, 6, 5, 4 and 3). The thickness of the membranes is controlled at 50-80 μm.

2. Characterization and measurements

Fourier transform infrared (FT-IR) spectra of quaternized imidazole-functionalized polyketone (QAAPIPK) were recorded using a Nicolet 6700 FTIR spectrometer (Thermo Fisher Scientific Inc., Waltham, MA, USA) at a resolution of 4 cm^{-1}, and the absorption spectra were recorded from 4000 cm^{-1} to 400 cm^{-1} in all total reflection (ATR) mode. ^{1}H NMR spectra was performed with Bruker AV III HD 400 MHz at room temperature, with tetramethylsilane as an internal standard, chloroform-d as solvent, DCM and HFIP as co-solvent. The field-emission scanning electron microscopy (SEM, FEI, Oregon, USA) was employed to detect the morphology of the membrane with the accelerated voltage of 5 kV. The microphase separation structures in the membranes were observed by atomic force microscope (AFM, Multimode 8, Bruker Corporation) working in tapping mode and a high-resolution transmission electron microscope (TEM, Tecnai G2 F20 S-TWIN, FEI Company, USA). The polyelectrolyte solution of 0.05 wt% QAAPIPK was added dropwise to the carbon film copper mesh. The infrared lamp was placed 20 cm above the copper mesh, and the copper mesh was baked for 10 min to volatilize the solvent. The obtained copper mesh sample was directly used for TEM observation. The average periodic size of ionic channels in membranes was studied by small-angle X-ray scattering (SAXS) at the beamline BL16B1 of the Shanghai Synchrotron Radiation Facility (SSRF, shanghai, China). The samples were placed normal to the direction of X-ray and wavelength of the monochromatic X-ray was 0.124 nm. The distance from specimens to X-ray CCD detector was 1870 mm for SAXS test. The mechanical properties were characterized by an Instron 5967 universal material testing machine, according to ASTM D638-10 with the 5 mm/min extension rate. and five samples were measured for each testing and the average results were recorded. The thermal stability of the membranes was characterized under a nitrogen atmosphere in the temperature range from 30 °C to 800 °C with the heating rate of 10 °C/min by a thermogravimetric analysis (TGA, Mettler Toledo TGA-2 system, Mettler Toledo Corp., Switzerland).

2.1. Elemental analyses

The molar ratio (x) of the reacted 1, 4-dicarbonyl units with imidazole group in PK chains was performed with elemental analyses (Elementar Vario EL, Germany), and the molar ratio in the polymer backbone was calculated by the following formula [1]:

$$x = \frac{NM_{w2}}{M_N n + N(M_{w2} - M_{w1})} \qquad (1)$$

where N represent the nitrogen content per gram obtained by elemental analysis, M_N is the atomic mass of nitrogen, n is the number of nitrogen atoms in the N-substituted pyrrole units (the 1, 4-dicarbonyl group after reaction), M_{w1} is the molecular weight of a converted 1, 4-dicarbonyl unit (469 g/mol for QAAPIPK) and M_{w2} is the molecular weight of the 1, 4-dicarbonyl in the polyketone backbone (113.7 g/mol for PK).

2.2. Linear swelling degree, water uptake and ion exchange capacity

One piece of QAAPIPK (1cm × 4cm) was completely immersed in deionized water at room temperature for 24 hours to remove impurities from the surface of the membrane. Then, the pieces of membrane were immersed in deionized water and kept for at least 3 hours at the temperature ranging from 30 °C to 80 °C. Afterwards, the change of mass and dimensional change of QAFPK-E/C were quickly measured after wiping with absorbent paper, and WU and LSD of the membranes were calculated using the follow equation (2) and (3):

$$WU = \frac{W_w - W_d}{W_d} \times 100\% \qquad (2)$$

where W_w and W_d are the mass of the membrane in the hydrated state and the dry state, respectively.

$$LSD = \frac{L_w - L_d}{L_d} \times 100\% \qquad (3)$$

where L_w and L_d are the length ($LSD_{\text{in-plane}}$) or thickness ($LSD_{\text{through-plane}}$) of the membrane under hydration conditions and dry conditions, respectively.

The ion exchange capacity (IEC) of the QAAPIPK was characterized by the classical back titration method. One piece of QAAPIPK membranes (1 cm × 4 cm) was immerged in a 1 mol/L NaCl aqueous solution at 80 ℃ for 36 hours. After drying at 60 °C under vacuum for 24 hours, the mass of the sample was recorded. Then, the dried sample was immersed in a 0.5 mol/L Na_2SO_4 aqueous solution for 24 hours to release Cl^- from the membrane. Afterwards, this solution was titrated with a 0.1 mol/L $AgNO_3$ aqueous solution in the presence of an indicator (K_2CrO_4). The IEC was calculated using the follow equation (4):

$$\text{IEC (mmol/g)} = \frac{V_{Ag^+}\text{(ml)} \times 0.1\ \text{mol/L}}{W_{Cl^-}\text{(g)}} \qquad (4)$$

where V_{Ag^+} is the dosage of $AgNO_3$ solution used during the titration, and W_{Cl^-} is the mass of the QAAPIPK membrane in the Cl^- form.

2.3. Hydroxide (OH-) conductivity

The hydroxide (OH^-) conductivity of all QAAPIPK was measured on the four-electrode AC impedance spectroscopy, which was obtained by an electrochemical workstation (CHI660E, Shanghai Chenhua). The potentiostat control mode was used to record the AC impedance spectrum over a frequency range from 0.1 MHz to 1 Hz with a perturbation voltage amplitude of 10 mV. The QAAPIPK membranes and electrodes were placed in a Teflon mold, and it measured in a thermal chamber of deionized water with a distance of 1 cm between the platinum black electrodes. The hydroxide conductivity (σ, mS/cm) was calculated using equation (5):

$$\sigma = \frac{L}{RWd} \qquad (5)$$

where L is the distance between the platinum black electrodes, R is the resistance of membrane, d was the thickness of the samples and W is the width of the membranes.

2.4. Single fuel cell performance testing

Alkaline single fuel cell performance of QAAPIPK-C (QAAPIPK-1-8-C and QAAPIPK-1-3-C) was characterized by a single cell test at 60 ℃. Firstly, a small amount of HFIP dissolved QAAPIPK-C ionomer was mixed with ethyl acetate. The catalyst (HPT020, 20% mass Pt/C, Shanghai Hesen Co. Ltd, China) was added to the solution and dispersed uniformly to obtain a catalyst ink. Afterwards, the catalyst ink was sprayed on the surface of the hydrophobic carbon paper to acquire a catalyst layer with a loading ratio of 0.4 mg/cm^2. QAAPIPK-C and two sheets of catalyst-containing paper were hot pressed to obtain a membrane electrode assembly (MEA). Finally, single alkaline cell fuel performance was carried out on a fuel cell test system (FCTS, ARBIN Instruments, USA) at 60 °C and 100% relative humidity. The flux rates of H_2 and O_2 gas attained 150 mL/min, and the relative gas humidity was 100%.

2.5. The contact angle and the stability of the contact angle

The contact angle tests were recorded on a DSA25 (Kruess Scientific Instruments, Germany), using water or oil droplet of 3-5 μL. The air medium and underwater contact angle tests are all done at room temperature. The water/oil contact angle in air medium, underwater contact angle, and underoil contact angle were all tested at room temperature.

The stability of the membrane was evaluated by studying the changes in the contact angle of the QAAIPPK-1-5-E under various working conditions. The QAAIPPK-E membranes were immersed in saturated NaCl aqueous solution, 1 M HCl aqueous solution, and 1 M NaOH aqueous solution under ultrasonic treatment respectively, and ultrasonic treatment was performed for 48 hours. Then, the membranes were washed several times with ethanol and deionized water in sequence, and dried under vacuum at 50 ℃ to completely remove the remaining solvent. The water contact angle (WCA), n-hexane contact angle (OCA), the underoil water contact angles (UOWCA), and the underwater oil contact angles (UWOCA) were tested.

2.6. Liquid flux performance and oil-water separation test

The pump-free natural fluxes of water, ethanol, acetone, ethyl acetate, chloroform, n-hexane and xylene in QAAPIPK-1-5 were tested. The flux test of each liquid was repeated 12 times continuously. The liquid flux of the QAAPIPK-1-5 membranes was obtained using equations (6):

$$\mathrm{Flux} = \frac{V}{AT} \qquad (6)$$

where V is the volume of liquid passing through the membrane in a certain period of time, A is the effective area of membranes (m^2), and T is the permeation time (hours).

The oil-water mixed solution was prepared by mixing 15 mL of organic solvent stained with Sudan III and 15 mL of water stained with methylene blue (MLB) directly. The surfactant-stabilized O/W emulsion was prepared by adding 1 mL of organic solvent to a homogeneous solution of 20 mg of emulsifier SDS and 100 mL of deionized water, and then stirring the mixture at 1500 rpm for 2 hours. The surfactant-stabilized W/O emulsion was prepared by adding 1 mL of water to a solution of 50 mg of emulsifier Span 80 and 100 mL of organic solvent, and then stirring the mixture at 1500 rpm for 2 hours. Under the action of gravity, 20 mL of oil-water mixed solution or surfactant-stabilized emulsion spontaneously passed through QAAPIPK-1-5 membrane with a thickness of 50 μm to test the flux and separation efficiency (SE) of it. The flux and separation efficiency of the membranes were obtained using equations (6) and (7), respectively:

$$\text{Separation efficiency (SE)} = \left(1 - \frac{Q_2}{Q_1}\right) \times 100\% \qquad (7)$$

Q_1 is the oil or water content in the pristine emulsion (mg/L), Q_2 is the oil/water content in the filtered water (mg/L). Total organic carbon analyzer (Germany, ELEMENTAR, Vario TOC) was employed to test the oil content in the pristine emulsion and filtered water. The distribution and droplet sizes of the pristine emulsions and the filtered oil or water after separation were observed by dynamic light scattering measurement ((DLS, BI-200SM, Brookhaven Instruments, USA) and Olympus BX51 polarizing optical microscopy (POM, Olympus Co., Tokyo, Japan).

2.7. Alkaline stability

In order to characterize the alkaline stability of the QAAPIPK, the samples of

QAAPIPK-AEM were immersed in a 1 mol/L KOH aqueous solution at 80 °C for different soaking time. Afterwards, the samples were repeatedly washed with deionized water to remove the residual KOH. The hydroxide conductivity of the QAAPIPK was measured again and compared with its initial value. Besides, the FTIR spectra of the samples after the alkaline resistance test was characterized to detect the changes in the chemical structure of QAAPIPK-AEM.

3. Figures and Tables

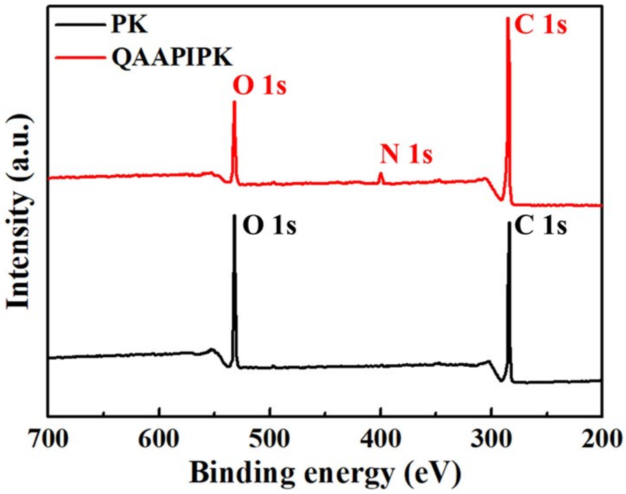

Figure S1. XPS total spectra of PK and QAAPIPK-1-8.

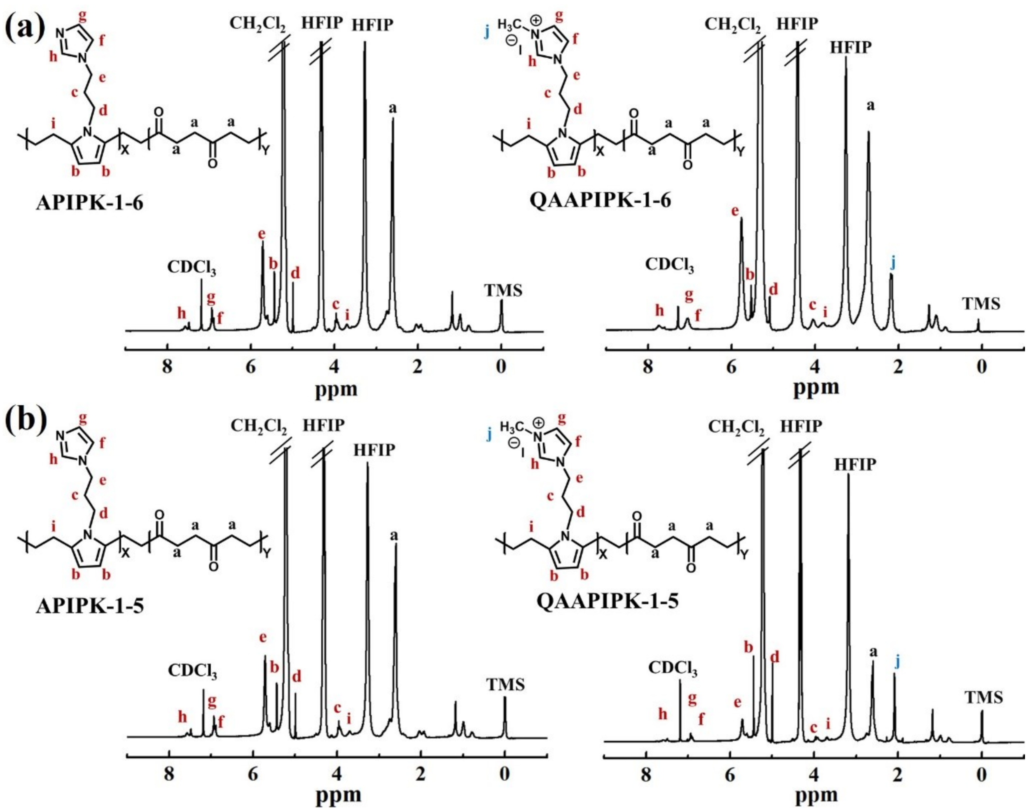

Figure S2. **(a)** ^{1}H NMR spectra of APIPK-1-6 and QAAPIPK-1-6. **(b)** ^{1}H NMR spectra of APIPK-1-5 and QAAPIPK-1-5.

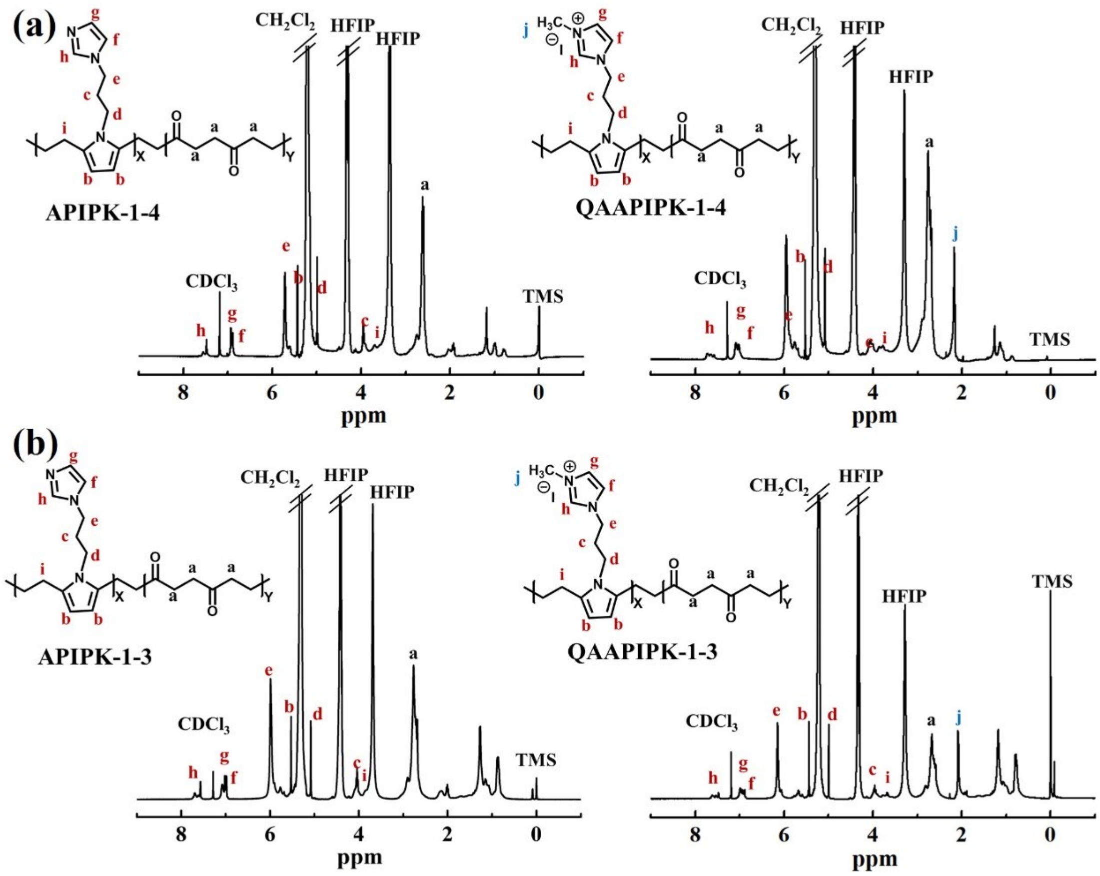

Figure S3. **(a)** ^{1}H NMR spectra of APIPK-1-4 and QAAPIPK-1-4. **(b)** ^{1}H NMR spectra of APIPK-1-3 and QAAPIPK-1-3.

Figure S4. Photographs of QAAPIPK-1-n-C (n=8, 6, 5, 4 and 3). The scale bar in the image is 1 cm.

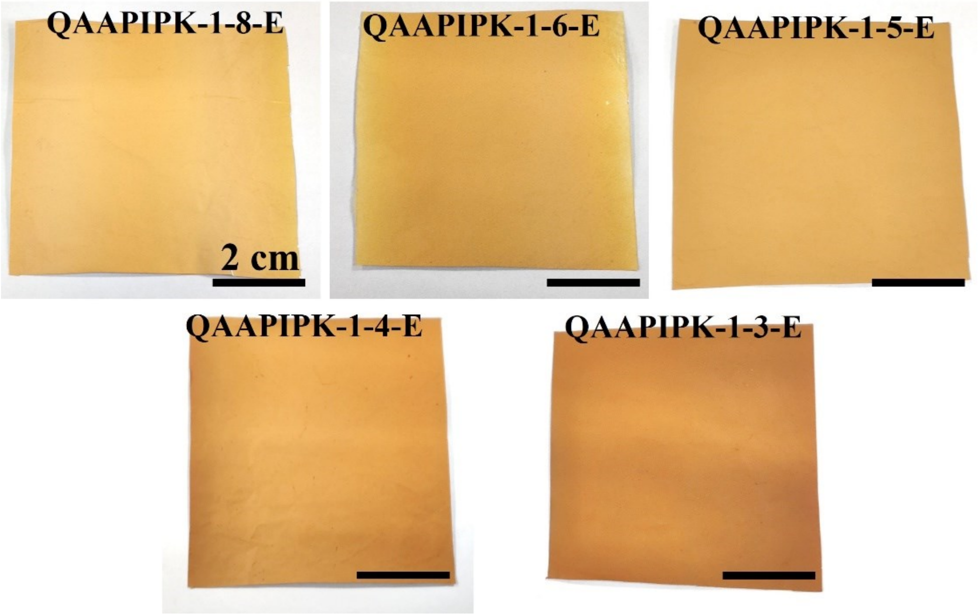

Figure S5. Photographs of QAAPIPK-1-n-E (n=8, 6, 5, 4 and 3). The scale bar in the image is 2 cm.

Table S1 Elemental composition of the QAAPIPK-1-n (n = 8, 6, 5, 4 and 3).

Samples	C %	H %	N %	X %	Z(X/1-X)
QAAPIPK-1-8	64.36	7.47	4.01	16.38	0.21
QAAPIPK-1-6	63.96	7.28	5.59	28.72	0.40
QAAPIPK-1-5	65.07	7.18	6.12	34.29	0.52
QAAPIPK-1-4	63.36	6.96	6.78	43.19	0.76
QAAPIPK-1-3	64.31	6.85	7.13	48.64	0.95

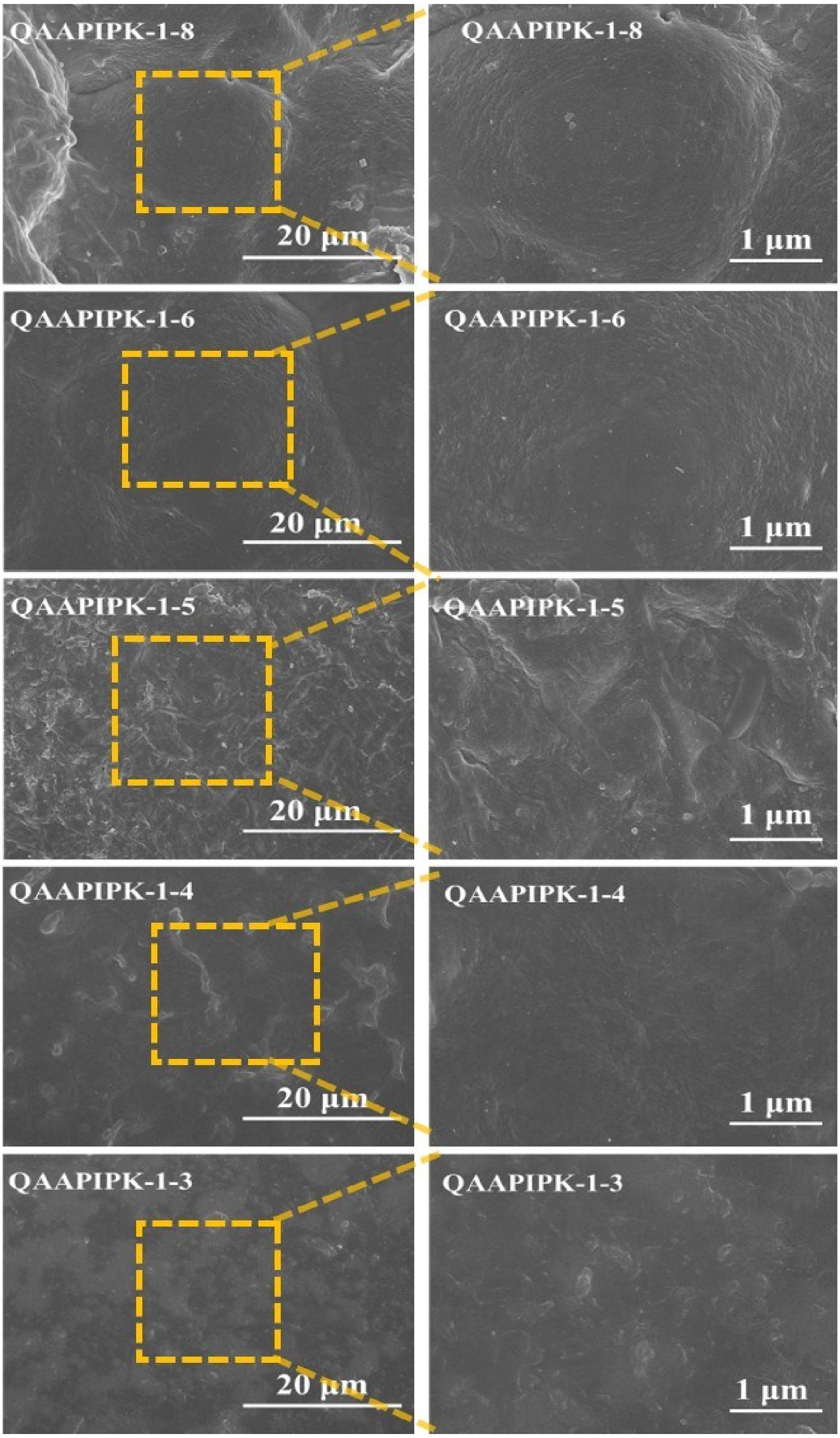

Figure S6. SEM images of surface morphology of the QAAPIPK-1-n-C (n = 8, 6, 5, 4 and 3).

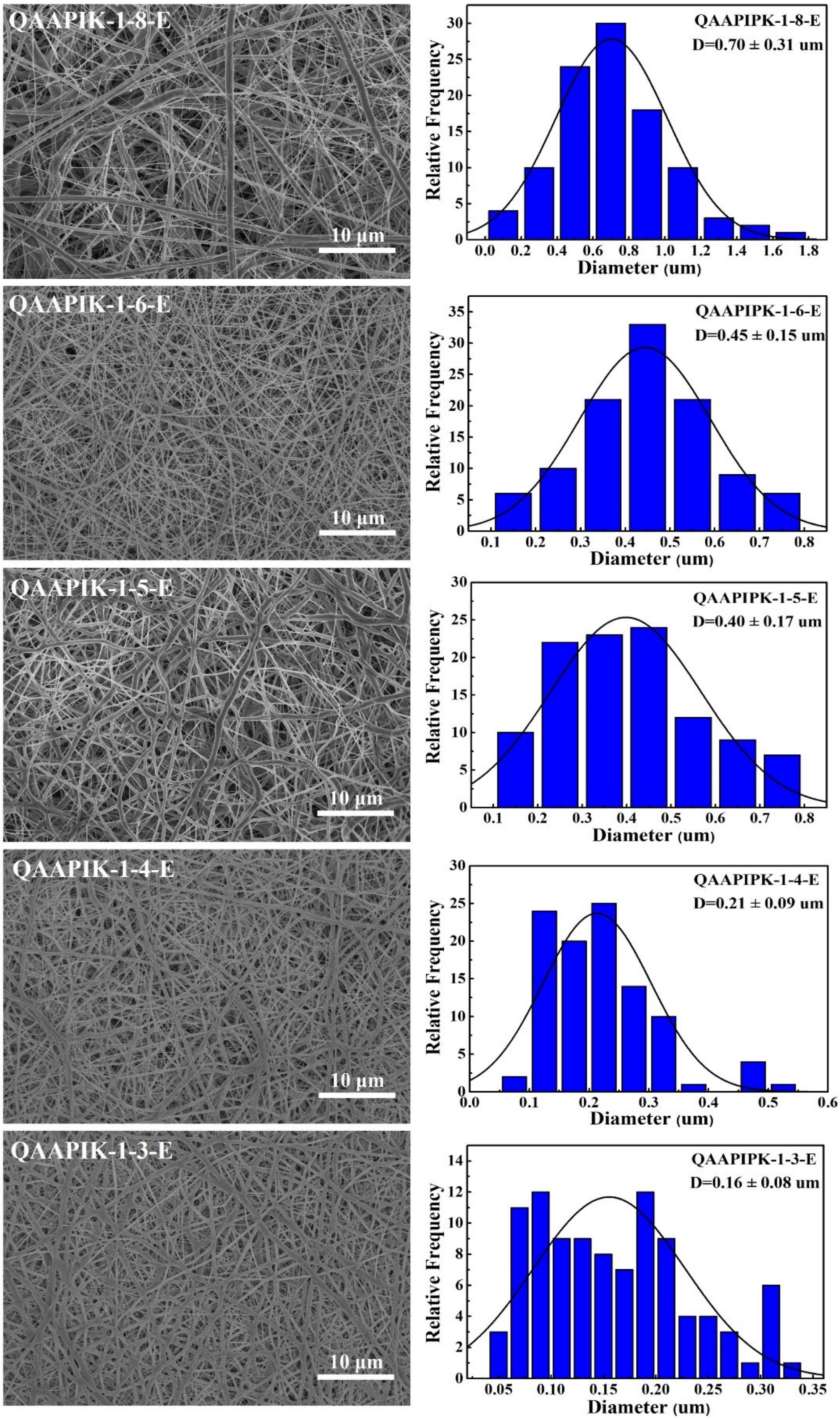

Figure S7. SEM images of surface morphology of the QAAPIPK-1-n-E (n = 8, 6, 5, 4 and 3), and the statistical distribution diagram of fiber diameter in QAAPIPK-1-n-E.

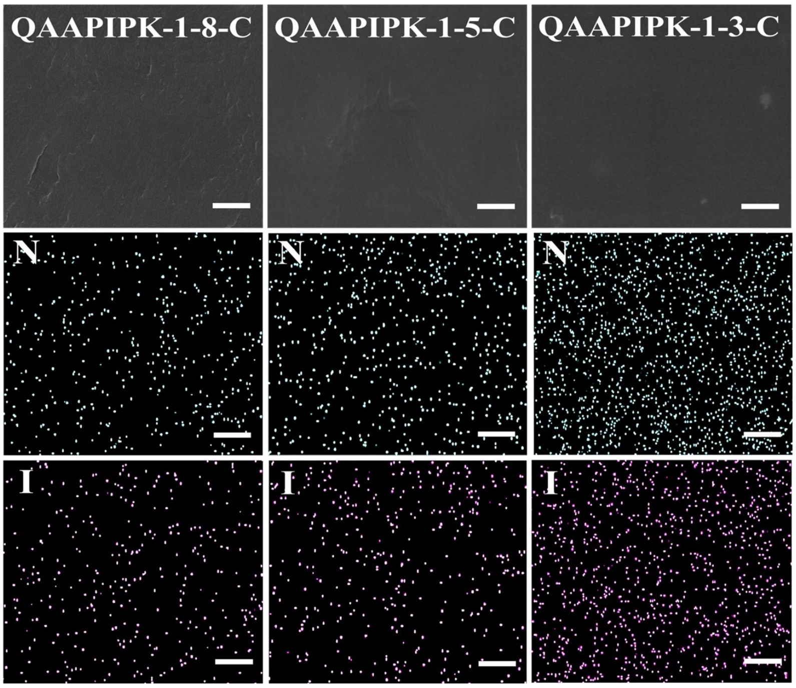

Figure S8. SEM cross-sectional image and mapping images of N and I element of QAAPIPK-1-n-C (N= 8,5 and 3), which QAAPIPK-C is in the state where the anion is iodide and the scale bar is **1 μm**.

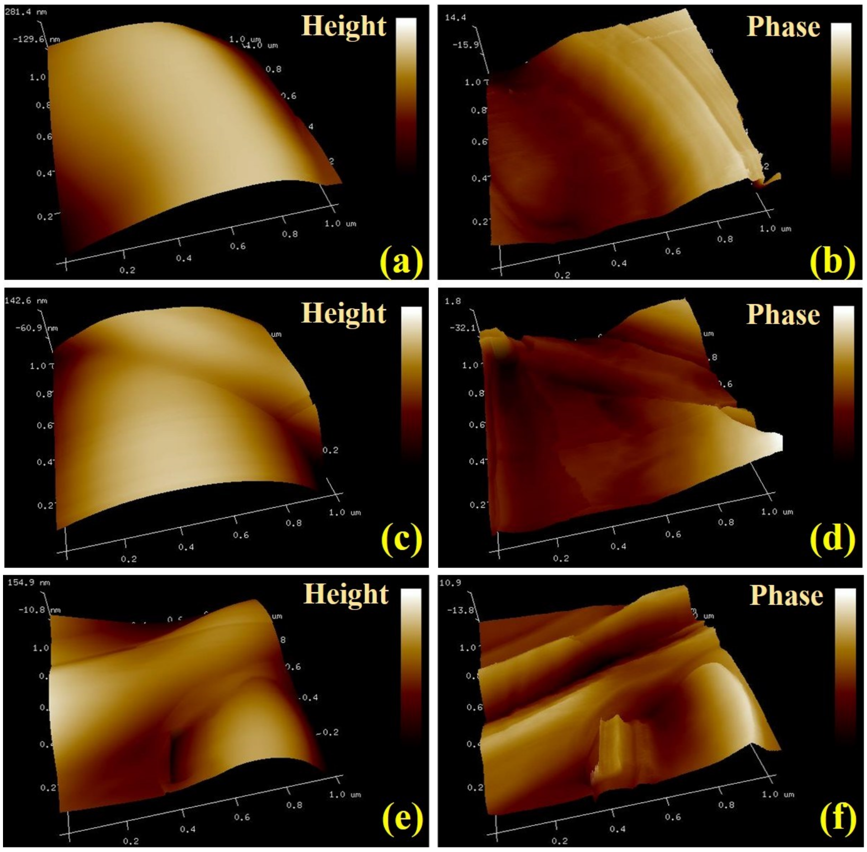

Figure S9. AFM height and phase images of single fiber in electrospun QAAPIPK-E. Height image: QAAPIPK-1-8-E (a), QAAPIPK-1-5-E (c) and QAAPIPK-1-3-E (e). Phase image: QAAPIPK-1-8-E (b), QAAPIPK-1-5-E (d) and QAAPIPK-1-3-E (f). The width size of images is 1 μm.

Table S2 The IEC of the QAAPIPK-1-n-C (n = 8, 6, 5, 4 and 3). The apparent activation energy (Ea) of the OH- conduction of QAAPIPK-1-n-C (n = 8, 6, 5, 4 and 3). The characteristic parameters (d) of ion clusters of QAAPIPK-1-n-C (n = 8, 6, 5, 4 and 3).

Samples	IEC (mmol/g)	Ea (kJ/mol)	d_1 (nm)	d_2 (nm)
QAAPIPK-1-8-C	1.64	14.8	6.97	7.8
QAAPIPK-1-6-C	1.81	14.1	7.30	8.6
QAAPIPK-1-5-C	1.99	13.9	9.62	11.4
QAAPIPK-1-4-C	2.36	13.6	10.81	13.0
QAAPIPK-1-3-C	2.46	12.8	12.57	15.3

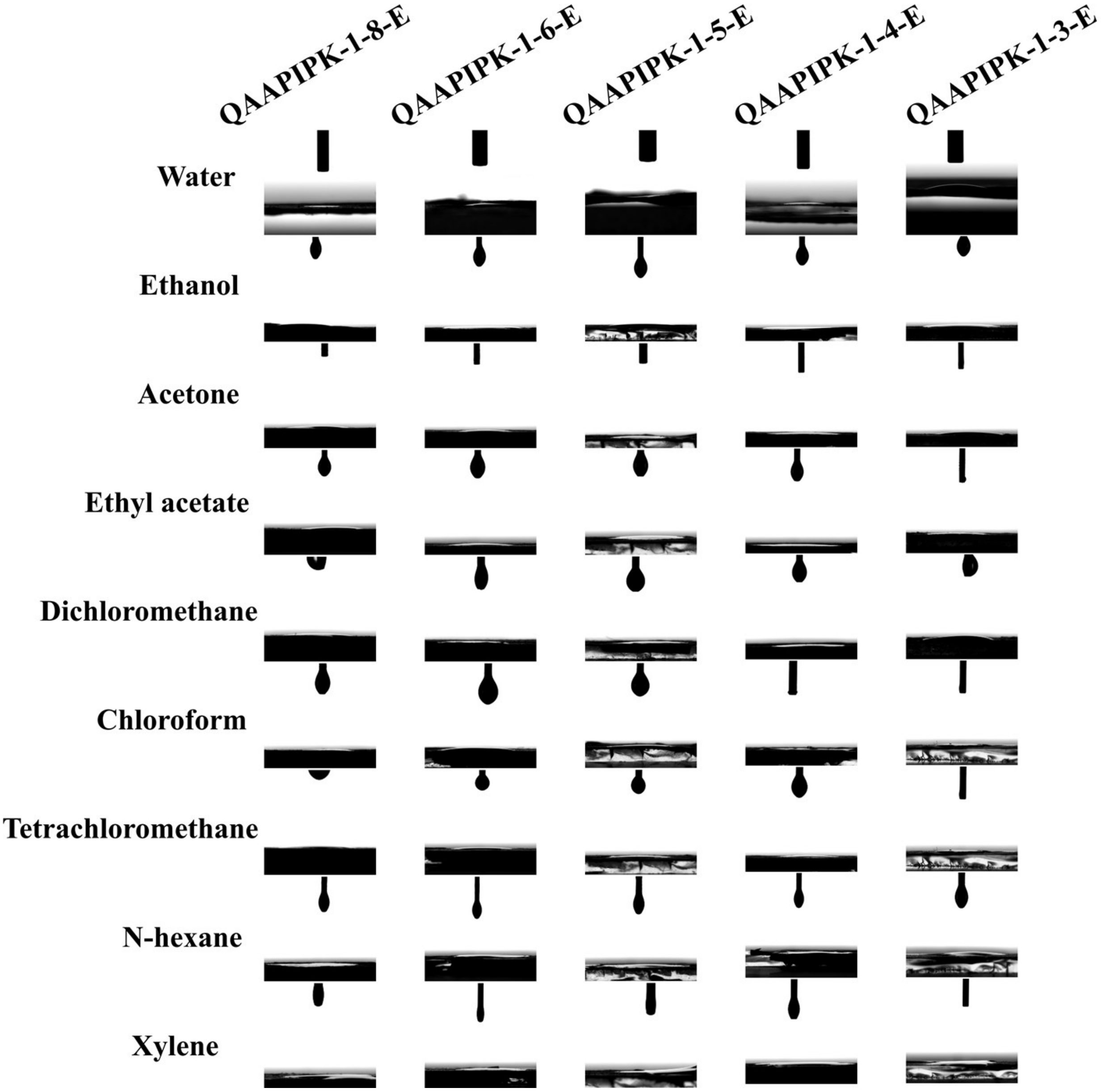

Figure S10. Water/oil contact angle images of various liquids (such as water, ethanol, acetone, ethyl acetate, dichloromethane, chloroform, tetrachloromethane, n-hexane and xylene) dropped on the samples of QAAPIPK-1-n-E (n = 8, 6, 5, 4 and 3) within one second.

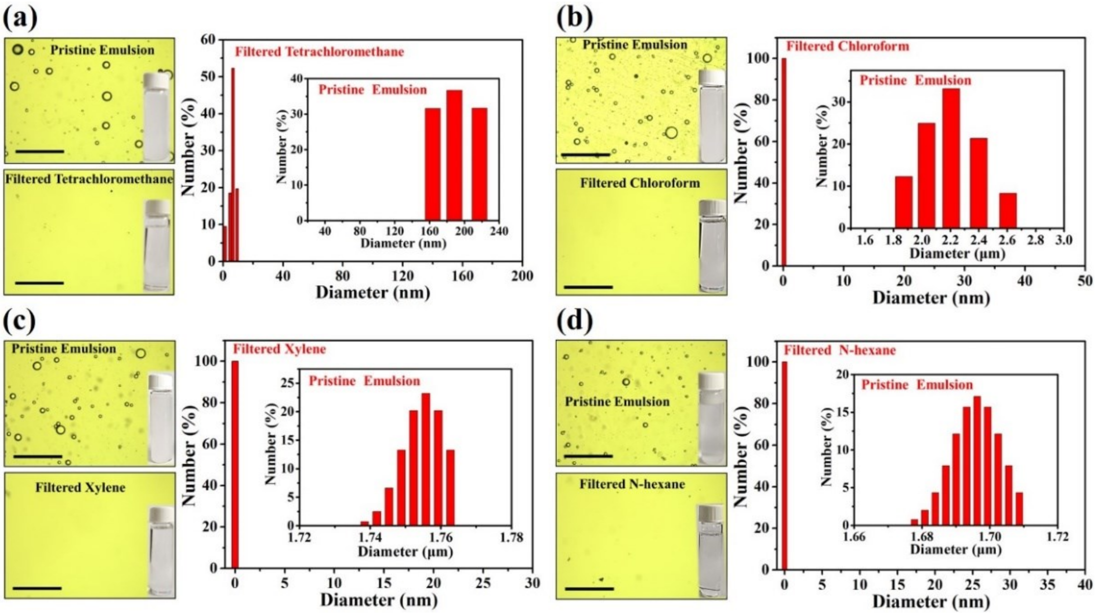

Figure S11. Optical microscope (OM) photographs and dynamic light scattering (DLS) images before and after filtration by the QAAPIPK-1-5-E for the water-in-oil emulsion. The top and down OM images are the pristine oil-in-water emulsion and filtered oil/solvent without water, respectively, and the insets are the digital picture of the pristine emulsion before and after filtration. The black scale bar in the inset is 5 μm. The image on the outside is the DLS data of the collected filtered oil/solvent after separation, and the inset is the DLS data of the pristine emulsion before filtration. Water-in-tetrachloromethane emulsion **(a)**, water-in-chloroform emulsion **(b)**, water-in-xylene emulsion **(c)** and water-in-n-hexane emulsion **(d)**.

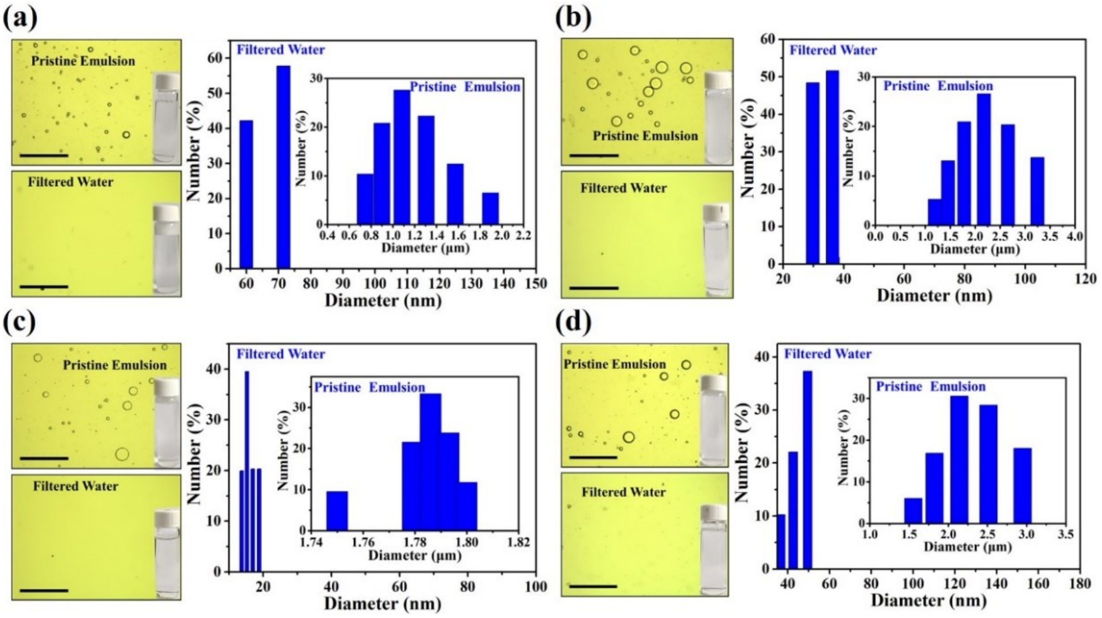

Figure S12. Optical microscope (OM) photographs and dynamic light scattering (DLS) images before and after filtration by the QAAPIPK-1-5-E for the oil-in-water emulsion. The top and down OM image are the pristine oil-in-water emulsion and filtered water without oil/solvent, respectively, and the insets are the digital picture of the pristine emulsion before and after filtration. The black scale bar in the inset is 5 μm. The image on the outside is the DLS data of the collected filtered water after separation, and the inset is the DLS data of the pristine emulsion before filtration. Tetrachloromethane-in-water emulsion **(a)**, chloroform-in-water emulsion **(b)**, xylene-in-water emulsion **(c)** and n-hexane-in-water emulsion **(d)**.

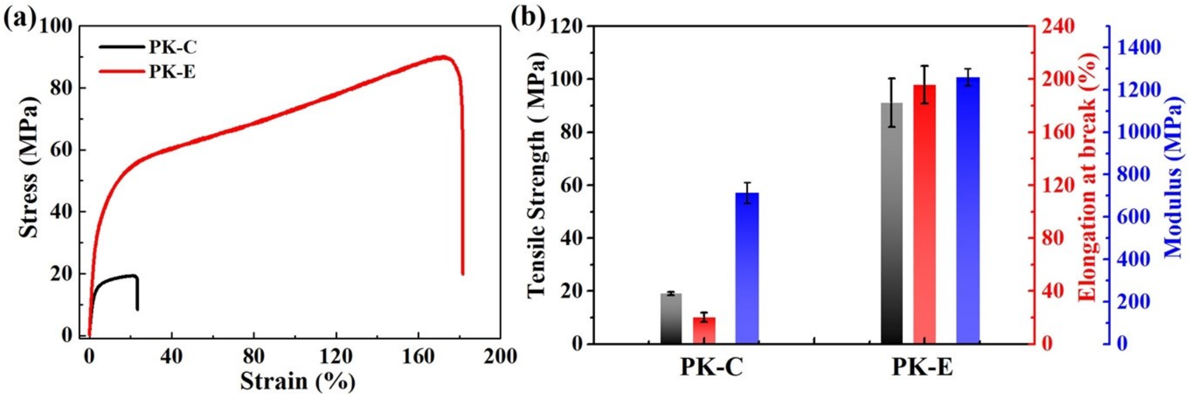

Figure S13. (a) Stress-strain curves of PK-C and PK-E. (b) The mechanical properties of PK-C and PK-E include tensile strength, elongation at break and tensile modulus.

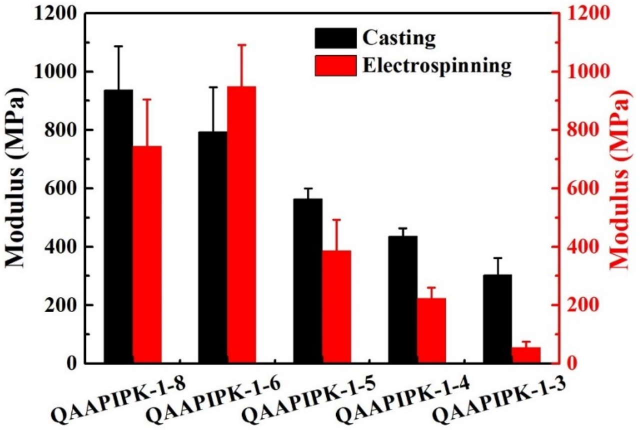

Figure S14. Elastic modulus of QAAPIPK-1-n-C and QAAPIPK-1-n-E (n = 8, 6, 5, 4 and 3).

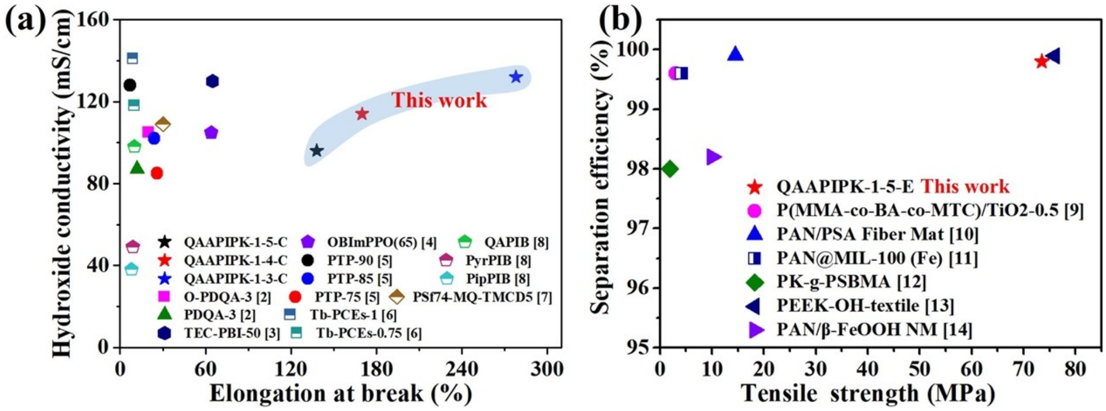

Figure S15. The comparison of the performance of QAAPIPK-C and QAAPIPK-E with the literature work in recent years. (a) Taking the elongation at break and the hydroxide ion conductivity as indicators, the comparison of QAAPIPK-1-5-C, QAAPIPK-1-4-C and QAAPIPK-1-3-C with the literature work in recent years.[2-8] (b) Taking tensile strength and oil-water separation efficiency as indicators, the comparison between QAAPIPK-1-5-E and the literature work in recent years.[9-14]

4. References

1 C. Toncelli, J. P. Pino-Pinto, N. Sano, F. Picchioni, A. A. Broekhuis, H. Nishide and I. Moreno-Villoslada, *Dyes Pigm.*, 2013, **98**, 51-63.
2 J. Zhang, K. Zhang, X. Liang, W. Yu, X. Ge, M. A. Shehzad, Z. Ge, Z. Yang, L. Wu and T. Xu, *J. Mater. Chem. A*, 2021, **9**, 327-337.
3 X. Wang, W. Chen, T. Li, X. Yan, Y. Zhang, F. Zhang, X. Wu, B. Pang, J. Li and G. He, *J. Mater. Chem. A*, 2021, **9**, 7522-7530.
4 Y. Zhu, L. Ding, X. Liang, M. A. Shehzad, L. Wang, X. Ge, Y. He, L. Wu, J. R. Varcoe and T. Xu, *Energy Environ. Sci.*, 2018, **11**, 3472-3479.
5 X. Hu, Y. Huang, L. Liu, Q. Ju, X. Zhou, X. Qiao, Z. Zheng and N. Li, *J. Membrane Sci.*, 2021, **621**, 118964.
6 Q. Yang, Y. Y. Cai, Z. Y. Zhu, L. X. Sun, Y. S. L. Choo, Q. G. Zhang, A. M. Zhu and Q. L. Liu, *ACS Appl. Mater. Interfaces*, 2020, **12**, 24806-24816.
7 L. Ma, N. A. Qaisrani, M. Hussain, L. Li, Y. Jia, S. Ma, R. Zhou, L. Bai, G. He and F. Zhang, *J. Membrane Sci.*, 2020, **607**, 118190.
8 S. Zhang, X. Zhu and C. Jin, *J. Mater. Chem. A*, 2019, **7**, 6883-6893.
9 L. Ma, Y. Chen and J. Zheng, *Journal of Materials Science*, 2021, **56**, 11335-11351.
10 Z. Zhu, W. Wang, D. Qi, Y. Luo, Y. Liu, Y. Xu, F. Cui, C. Wang and X. Chen, *Adv. Mater.*, 2018, **30**, e1801870.
11 R. Zhao, Y. Tian, S. Li, T. Ma, H. Lei and G. Zhu, *J. Mater. Chem. A*, 2019, **7**, 22559-22570.
12 L. Zhang, Y. Lin, L. Cheng, Z. Yang and H. Matsuyama, *J. Membrane Sci.*, 2019, **582**, 48-58.
13 J. Wang, Y. Sun, W. Bi, Z. Jiang, M. Zhang and J. Pang, *J. Membrane Sci.*, 2020, **616**.
14 L. Zhang, Y. He, L. Ma, J. Chen, Y. Fan, S. Zhang, H. Shi, Z. Li and P. Luo, *ACS Appl. Mater. Interfaces*, 2019, **11**, 34487-34496.